MULTIVARIATE TIME SERIES ANALYSIS OF SOLAR IRRADIANCE FOR PHOTOVOLTAIC SYSTEMS: THE HYBRIDIZATION OF NARX AND LSTM MODELS

OSAMA GAMAL MAHMOUD IBRAHIM MOTIR

A thesis submitted in fulfilment of the
requirements for the award of the degree of
Master of Data Science

Faculty of computing
Universiti Teknologi Malaysia

NOVEMBER 2024

CHAPTER 3

RESEARCH METHODOLOGY

3.1 Introduction

This chapter outlines the comprehensive research methodology applied to achieve the objectives of this study, which focuses on improving solar irradiance forecasting through the hybridization of NARX and LSTM models. Research methodology serves as a systematic framework of rules, procedures, and techniques to guide the research process and ensure its alignment with the objectives established in Chapter 1. Selecting an appropriate methodology is critical to effectively navigate the various phases required to answer the research questions.

This chapter presents a detailed account of the methods and instruments used in this study, offering a clear picture of the entire process. It includes discussions on the identification and analysis of forecasting parameters, the collection and preprocessing of meteorological data, and the development and optimization of the hybrid NARX-LSTM model. Additionally, the chapter elaborates on the input sensitivity analysis and evaluation metrics employed to validate the model's performance. Each stage of the research process is systematically addressed to ensure the reliability and effectiveness of the proposed forecasting framework.

3.2 Research Framework

The methodology unfolds across a series of systematically designed stages as shown in Figure 3.1, each integral to the progression and integrity of the research. The approach commences with the identification of pivotal weather parameters essential for precise solar irradiance forecasting. This initial phase involves a meticulous analysis of various meteorological variables and their potential impact on forecasting

accuracy, underpinned by a thorough review of relevant literature and domain expertise.

Subsequently, the focus shifts to the selection of an appropriate machine learning model. The decision to employ a hybrid NARX-LSTM model is grounded in its theoretical suitability for capturing the complex, nonlinear relationships inherent in meteorological data and its proven efficacy in time-series forecasting. Undergoes a preliminary stage of model tuning and input sensitivity analysis. This tuning optimizes the model's performance, addressing the balance between accuracy and computational demands. The input sensitivity analysis, conducted prior to the training phase, assesses the impact of each weather parameter on the model's output, providing insights into the relative importance of each variable.

Following model selection, the methodology advances into the data collection phase. Here, the specifics of data collocation, including the choice of Johor Bahru, Malaysia, as the geographical focus. The chapter will detail the process of gathering, cleaning, and preprocessing the data, ensuring its alignment with the identified forecasting parameters and its readiness for model training.

The subsequent stage encompasses the training of the NARX-LSTM model, where the nuances of network architecture, training protocols, and optimization strategies are expounded. The validation of this model is critical and is conducted using robust statistical methods to assess and ensure its predictive performance.

The final stage culminates in the result validation process. Here, the outputs of the NARX-LSTM model are meticulously cross-verified against actual meteorological data to evaluate the accuracy and reliability of the forecasts. Additionally, a comparative analysis with standalone models is conducted, showcasing the hybrid model's enhanced predictive capabilities and efficiency. This stage is pivotal in affirming the effectiveness of the hybrid model and its applicability in real-world scenarios.

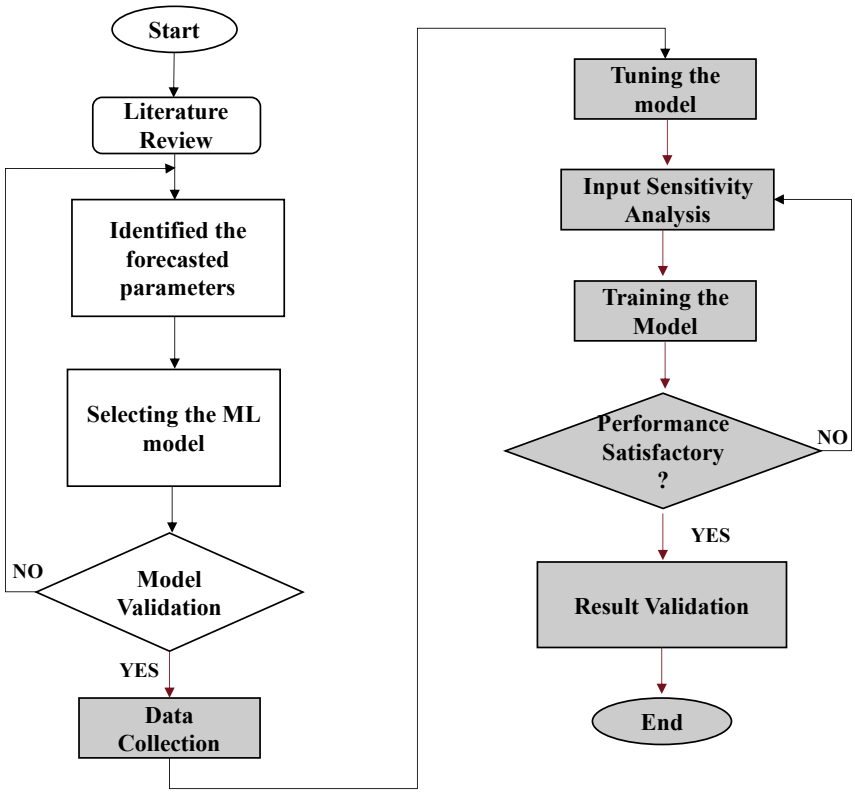

Figure 3.1 Methodology Flowchart

3.3 Data Analysis

This section comprehensively outlines the systematic procedures undertaken to transform raw meteorological data into an optimized dataset suitable for accurate solar irradiance forecasting. It begins with the identification of key forecast parameters, a process that integrates insights from literature review and domain expertise to determine the most influential meteorological factors affecting solar irradiance. These parameters form the foundation of the forecasting model, ensuring it captures the critical interactions between environmental variables and solar energy dynamics.

Following parameter identification, the data analysis process progresses to data collection, where historical meteorological data spanning a significant temporal range is gathered. This data is meticulously sourced to ensure accuracy, reliability, and

relevance to the study's geographical focus. The collected dataset is then subjected to a comprehensive preprocessing phase, which includes data cleaning, normalization, and feature engineering. These steps address inconsistencies, scale differences, and the temporal characteristics of the data, ensuring its readiness for effective model training.

Moreover, this section delves into the exploration of data distributions and relationships through histograms and scatter plots, providing valuable insights into the behavior of the meteorological variables over time. These analyses not only guide the preprocessing techniques but also highlight seasonal and diurnal trends that are critical for time-series forecasting. The structured approach detailed in this section lays the groundwork for developing a robust and reliable predictive model, enabling the effective forecasting of solar irradiance under varying environmental conditions.

3.3.1 Identification of Forecast Parameters

The Identification of Forecast Parameters phase integrates detailed data analysis with comprehensive literature review. This stage finalizes the meteorological parameters crucial for forecasting solar irradiance: air temperature, cloud attenuation, precipitation rate, precipitable water, relative humidity, air pressure, wind direction, wind speed, and dewpoint temperature. These variables are pivotal due to their substantiated effect on solar energy as identified through historical data trends. This meticulous selection process ensures that the forecasting model incorporates the most significant and impactful weather elements.

Air temperature is a critical factor, as it directly correlates with the efficiency of photovoltaic cells, influencing the overall solar energy generation. Cloud attenuation is pivotal due to its impact on the amount of solar radiation reaching the Earth's surface, directly affecting the variability of solar irradiance. The role of precipitation rate is highlighted in research exploring its effects on solar irradiance levels during rainfall events, while precipitable water in the atmosphere is key due to its role in absorbing and scattering sunlight, impacting the solar irradiance levels. Relative humidity, indicative of atmospheric moisture, influences cloud formation and

the diffusion of solar radiation. Air pressure, a determinant of weather patterns, affects the clarity of the sky and, consequently, solar irradiance. Wind direction and speed are included for their roles in cloud movement and the dispersal of airborne particulates, which can significantly alter the atmospheric clarity and solar radiation reception. Finally, dewpoint temperature is considered for providing insights into atmospheric moisture levels, thus influencing potential cloud cover and solar irradiance.

The selection of these parameters is supported by their established impact on various aspects of solar energy dynamics and a comprehensive review of existing literature, ensuring that the chosen variables are not only relevant but also empirically validated for their influence on solar irradiance forecasting. Understanding these influences is crucial for accurately predicting solar irradiance, as they collectively embody the complex interactions within the Earth's atmosphere that affect solar energy generation. This careful identification of forecast parameters forms the foundation for the subsequent modeling and analysis, ensuring a comprehensive approach to predicting solar irradiance.

Incorporating the relationship between various weather parameters and solar irradiance or Global Horizontal Irradiance (GHI) into the Identification of Forecast Parameters phase enriches the model's contextual understanding as evidenced in Figure 3.2. Air temperature shows a positive correlation with GHI, suggesting sunnier conditions with rising temperatures. While dewpoint temperature has a moderate positive correlation, its subtler influence compared to air temperature is noted. Precipitation rate's slight positive relationship with GHI indicates that intermittent rain doesn't always hinder solar irradiance. Surface pressure's weak positive trend aligns with the expectation of higher GHI during high-pressure conditions, indicative of clear skies.

Conversely, precipitable water's negative correlation implies potential cloud formation that may reduce GHI. Cloud opacity strongly inversely affects GHI, affirming its role in blocking sunlight. Lastly, relative humidity strongly negatively correlates with GHI, typically signaling overcast conditions leading to reduced solar exposure. These relationships underscore the complexities of predicting solar

irradiance and the need for a nuanced model that accounts for these varied meteorological impacts.

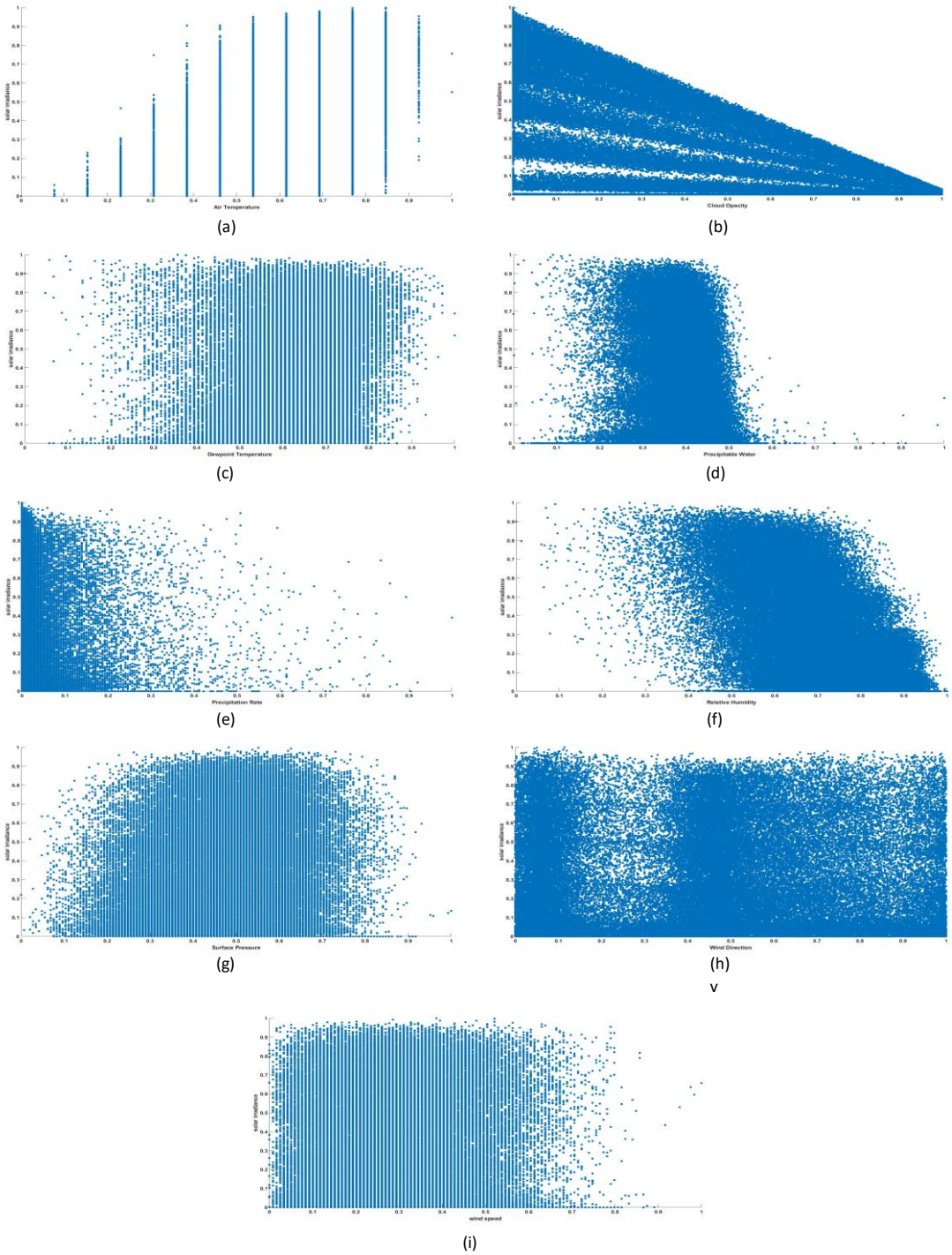

Figure 3.2 scatter plots of (a) Air Temperature, (b) Cloud Opacity, (c) dewpoint temperature, (d) precipitable water, (e) precipitation rate, (f) relative humidity,(g) Surface Pressure, (h) Wind Direction and (i) wind speed - against the SI.

3.3.2 Data Collection

Following the meticulous identification of forecast parameters, the research progresses to the data collection phase. This critical stage involves the systematic collection of data corresponding to the identified meteorological variables, essential for the effective forecasting of solar irradiance.

The data encompasses a comprehensive range of parameters including air temperature, cloud attenuation, precipitation rate, precipitable water, relative humidity, air pressure, wind direction, wind speed, and dewpoint temperature as can be seen in Figure 3.3. This dataset is sourced from Det Norske Veritas (DNV), a globally recognized authority in quality assurance and risk management, ensuring the reliability and accuracy of the information. The data spans from January 1, 2007, to November 29, 2023, providing a substantial temporal coverage that enhances the robustness of the analysis. The readings are recorded on an hourly basis, offering a detailed temporal resolution that is critical for capturing the nuances of solar irradiance variability.

Located in Johor Bahru, Johor, Malaysia, the geographical setting of the data collection is significant. The region's diverse climatic conditions present an ideal environment for studying the impacts of various environmental variables on solar irradiance. The hourly readings, encompassing a wide array of weather conditions over an extended period, provide a rich dataset that is instrumental in developing a nuanced and comprehensive forecasting model.

The meticulous approach to data collection, emphasizing both the quality and the scope of the data, lays a solid foundation for the subsequent stages of preprocessing and analysis. By ensuring the data's accuracy and relevance, this phase plays a pivotal role in the overall success of the research, enabling the development of a reliable and effective solar irradiance forecasting mode.

air_temp	cloud_opa	dewpoint	ghi	precipitab	precipitat	relative_h	surface_p	wind_dire	wind_spe	period_end
25	59.1	23.3	101	53.6	0	91.7	1004.1	316	3.8	2007-01-01T01:00:00Z
26	55	23.9	213	53.9	0	90.3	1004.8	313	3.4	2007-01-01T02:00:00Z
27	56	24.2	296	54.3	0	86.2	1005.2	317	3.6	2007-01-01T03:00:00Z
28	43	24.1	468	54.9	0	81	1005.2	324	4	2007-01-01T04:00:00Z
29	7.6	24.1	832	55.8	0	76	1004.7	327	4.1	2007-01-01T05:00:00Z
30	0	24.3	910	56.7	0.1	73.7	1003.9	328	4.2	2007-01-01T06:00:00Z
29	9.8	23.6	766	57.3	1.9	73.8	1003.1	327	4.2	2007-01-01T07:00:00Z
27	17.4	22.8	595	56.8	0.5	75.8	1002.1	335	4	2007-01-01T08:00:00Z
27	47.8	23.3	285	56.3	0.3	80.5	1001.4	346	4	2007-01-01T09:00:00Z
27	75.9	23.7	77	56.7	0.2	83.4	1001.6	343	3.9	2007-01-01T10:00:00Z
26	49.7	23.6	41	57.4	0.2	84.9	1002.4	339	3.8	2007-01-01T11:00:00Z
26	67	23.5	0	57.7	0.1	86.1	1003.2	340	3.7	2007-01-01T12:00:00Z
26	69.3	23.5	0	58	0.1	87.2	1004.1	332	3.9	2007-01-01T13:00:00Z
26	55.7	23.5	0	58.7	0.1	88.7	1004.9	317	4.6	2007-01-01T14:00:00Z
25	50.9	23.5	0	59.3	0.1	90.9	1005.4	308	4.9	2007-01-01T15:00:00Z
25	49.6	23.4	0	59.9	0	92.2	1005.6	301	4.7	2007-01-01T16:00:00Z
25	36.3	23.4	0	60.3	0.1	92.8	1005.5	301	4.6	2007-01-01T17:00:00Z
25	32.5	23.3	0	60.1	0.1	93	1004.9	299	4.6	2007-01-01T18:00:00Z
25	47.7	23.3	0	59.8	0	93	1004.2	288	5	2007-01-01T19:00:00Z
25	51.5	23.2	0	60	0	93	1003.5	282	5.5	2007-01-01T20:00:00Z
24	46.1	23.3	0	60.2	0.1	93.6	1003.1	286	5.6	2007-01-01T21:00:00Z
25	48	23.4	0	59.2	0.4	93.6	1003.3	300	5	2007-01-01T22:00:00Z
24	32.6	23.2	0	58.3	0.2	93	1003.5	309	4.6	2007-01-01T23:00:00Z

Figure 3.3 Historical data for 24 hours - January 1, 2007

3.3.3 Data Preprocessing

The data preprocessing stage is integral to the structuring of meteorological data for analysis and modeling. This phase commences with a thorough examination of variable histograms to distill key insights from data distributions. These insights underpin systematic procedures to rectify inconsistencies, normalize variable scales, and structure time-series data, ensuring the dataset's readiness for predictive modeling. The histogram analysis is pivotal, as it informs the treatment of outliers, guides feature selection, and confirms the robustness of the data across temporal variations from 2007 to 2023.

The analysis of histogram distributions for meteorological variables offers a nuanced understanding of the data's behavior as shown in Figure 3.4. The air temperature histogram displays a multimodal distribution, indicating seasonal temperature fluctuations. Recognizing these peaks is vital as they directly influence solar panel efficiency. Similarly, the right-skewed cloud opacity histogram suggests more frequent clear skies with occasional dense cloud cover, a key variable in

predicting irradiance variability. Meanwhile, the dewpoint temperature’s normal distribution points to stable moisture conditions, affecting dew formation and subsequent solar irradiance levels.

Global Horizontal Irradiance (GHI) presents a pronounced left-skew, predominantly featuring lower irradiance values, which are essential in modeling the diurnal cycle and the impact of cloud coverage. Precipitable water's near-normal distribution underscores its role in the atmosphere's ability to absorb and scatter solar radiation, a significant factor in irradiance measurements.

The exponential decay observed in the precipitation rate histogram, where most data points indicate minimal precipitation, is crucial for modeling as heavy rainfall can significantly reduce irradiance. The left-skew in relative humidity, especially in higher values, reflects the humidity's impact on cloud formation and solar irradiance in tropical climates.

Surface pressure’s normal distribution suggests consistent atmospheric conditions, valuable for forecasting weather patterns that affect irradiance. Wind direction’s bimodal distribution can inform the model about prevalent wind patterns that influence cloud cover and irradiance levels. Lastly, the right-skewed wind speed histogram indicates generally low wind speeds but acknowledges the potential for occasional high-speed winds that could disperse clouds and particulates, affecting irradiance.

Each histogram informs specific aspects of the preprocessing, like outlier treatment and feature selection, ensuring the forecasting model is built on a dataset that accurately reflects environmental conditions.

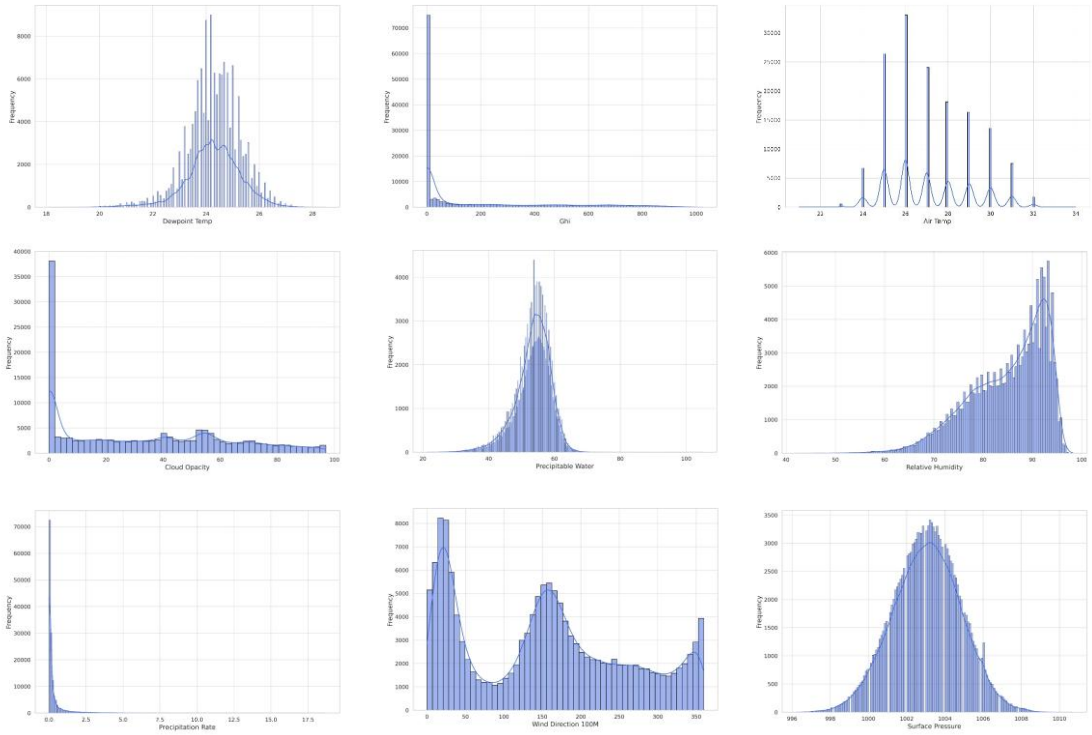

Figure 3.4 Histograms Distributions

During the data cleaning process, several inconsistencies and gaps were identified and rectified. The histograms distributions guided the data cleaning process, where outliers and anomalies were addressed. For instance, extreme values in cloud opacity and wind speed were capped to avoid undue influence on the model. Normalization was applied to standardize the range of independent variables, preserving their distributional characteristics without letting any single variable dominate due to scale differences. This was achieved using the Min-Max normalization method.

$$Normalized\ Value = \frac{Value - Min}{Max - Min} \tag{3.1}$$

This transformation scales the data within a range of 0 to 1, ensuring that each parameter contributes proportionately to the model's training process. Figure 3.5

illustrates this, demonstrating that the dynamics of the parameters remain consistent post-process.

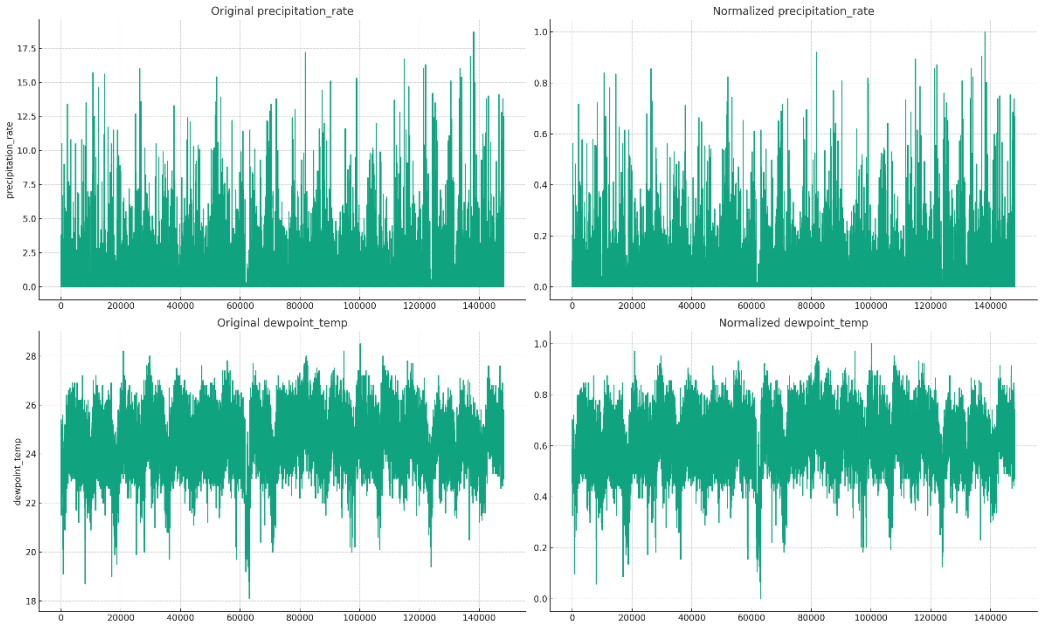

Figure 3.5 Comparison of Original and Normalized Meteorological Parameters

Feature engineering involved the incorporation of temporal patterns observed in the histograms in Figure 3.4, specifically the time of the month and hour of the day. These features were derived to capture the cyclical nature of solar irradiance across different timescales. This addition is expected to provide the model with finer granularity in understanding the diurnal and monthly variations in solar irradiance.

The data was divided into training, validation, and testing sets, with 70% allocated for training (spanning from 2007 to 2019), 15% for validation (covering 2020 to 2021), and 15% for testing (from 2022 to November 29, 2023). This partitioning was designed to provide a comprehensive training dataset while allowing for effective model validation and testing on more recent data, thereby ensuring the model's robustness and adaptability to recent climatic trends.

3.4 Model Development

The Model Development section comprehensively presents the structure and integration of the Nonlinear Autoregressive with Exogenous Inputs (NARX) neural network and the Long Short-Term Memory (LSTM) neural network, both of which are pivotal for enhancing the accuracy of solar irradiance forecasting. This section will elucidate the individual characteristics of the NARX and LSTM models, detailing their unique strengths in pattern recognition and temporal data analysis. Moreover, the synthesis of these models into a cohesive hybrid system is explored, highlighting the synergistic effects of this combination on forecasting proficiency. The section will also discuss the methodological steps taken to configure and optimize the hybrid model, ensuring that it not only captures the intricate dynamics of solar irradiance but also generalizes well to unseen data, thereby contributing to the advancement of predictive modeling in renewable energy systems.

3.4.1 Nonlinear Autoregressive with Exogenous Inputs (NARX) Neural Network:

The Nonlinear Autoregressive with Exogenous Inputs (NARX) Neural Network is a critical component of the hybrid NARX-LSTM model designed for solar irradiance forecasting. The NARX model excels in mapping the relationships between input and output time-series data, predicting future values based on this historical information. It operates on a functional relationship that involves both the external inputs $u(t)$ and the previous values of the output series $y(t)$. This capability makes the NARX model highly effective in capturing the non-linear dynamics often present in meteorological data, which is essential for accurate solar irradiance predictions. The standard form of the NARX model is given by:

$$y(t) = f\left[\left(y(t-1)\right),..,y\left(t-d_y\right),u(t),u(t-1),..,u(t-d_u)\right] \qquad (3.2)$$

where in the given text, $u(t)$ and $y(t)$ within the real number set represent the input and output of the model at a specific discrete time step, t respectively. This model includes a feedback loop which serves to enhance the model's responsiveness to past data. Figure 3.6 provides a visual representation of how the NARX algorithm functions.

As depicted in Figure 3.6, the NARX algorithm is composed of a two-layer feed-forward network. This includes a linear transfer function in the output layer and a sigmoid function (σ) in the hidden layer, as calculated and described in [80].

$$\sigma(\mathrm{x}) = \frac{1}{1 + \exp(-\sigma)} \tag{3.3}$$

A typical NARX neural network includes an input layer, one or more hidden layers with a nonlinear activation function (commonly a hyperbolic tangent sigmoid function), and a linear output layer. The network incorporates feedback connections from both the output and input layers via tapped delay lines that store previous values of the input $u(t)$ and output $y(t)$ sequences.

The input to the hidden layer at any time t is a combination of the current and delayed inputs, as well as the feedback from the previous outputs. The output of the network at time t, denoted by $\hat{y}(t)$, is then calculated as follows: is then calculated as follows:

$$\hat{y}(t) = W_o H + b_o \tag{3.4}$$

The NARX network is typically trained using a variant of the backpropagation algorithm, such as the Levenberg-Marquardt algorithm, which is well-suited for nonlinear least squares problems. During training, the network operates in an open-loop mode, using actual past output data for the feedback connections. Once trained, the network can be switched to a closed-loop mode for simulation, using its own predictions as feedback to generate future outputs as shown in Figure 3.7.

Despite its advantages, the NARX neural network's efficiency can be further enhanced by omitting the retention of past outputs, which notably diminishes the computational demand. However, as a variant within the recurrent neural network (RNN) family, the NARX model is not entirely immune to the vanishing gradient phenomenon. This issue arises when, beyond a certain number of inputs, the RNN ceases to retain new information, leading to a plateau in learning and, consequently, a decline in predictive precision. Such a challenge is manifested during the training phase, particularly when gradient descent algorithms begin to falter in maintaining the influence of input data over extended sequences, resulting in what is known as the diminishing memory problem.

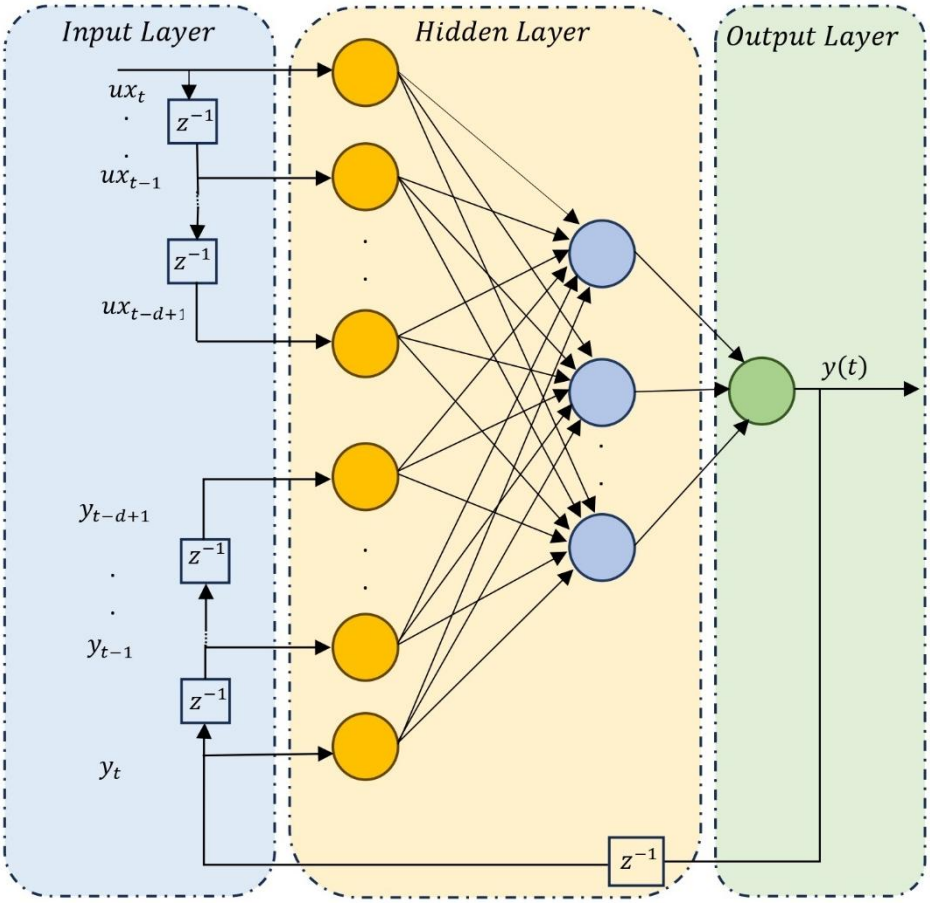

Figure 3.6 The architecture of the three-layered NARX

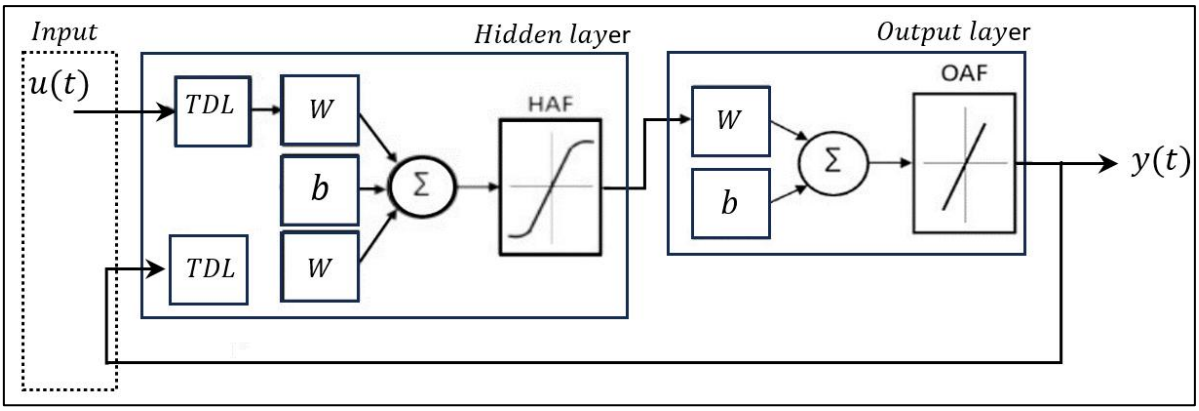

Figure 3.7 The architecture of the NARX

3.4.2 Long Short-Term Memory (LSTM) Neural Network

The LSTM network is an advanced architecture within the family of recurrent neural networks (RNNs), specifically designed to address the vanishing gradient problem that impedes the training of traditional RNNs. This architecture is characterized by its capacity to maintain long-term dependencies, a critical feature for tasks such as time-series forecasting where the significance of historical data extends over long periods.

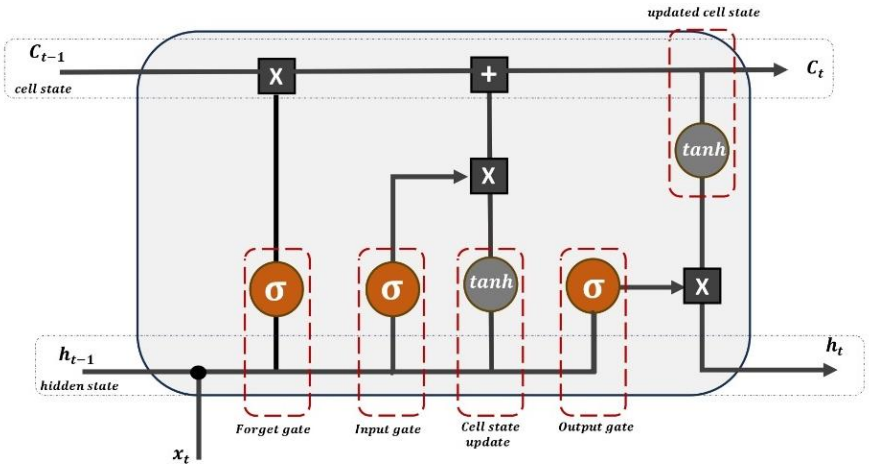

Figure 3.8 The architecture of the LSTM network

At the heart of the LSTM network lies the LSTM cell, which orchestrates the data flow through a sophisticated gating mechanism, as illustrated in Figure 3.8. Each cell consists of four integral components: the input gate (i_t), the forget gate(f_t), the output gate (o_t), and the cell state (C_t) which collectively manage the cell's memory. This mechanism enables them to preserve important long-term information and discard irrelevant data, a process formalized by the following set of equations:

$$i_t = \sigma(W_i[h_{t-1}, x_t] + b_i) \tag{3.5}$$

$$f_t = \sigma\big(W_f[h_{t-1}, x_t] + b_f\big) \tag{3.6}$$

$$\widetilde{C_t} = \tanh(W_C[h_{t-1}, x_t] + b_C) \tag{3.7}$$

$$C_t = f_t * \big([C_{t-1}, i_t] * \widetilde{C_t}\big) \tag{3.8}$$

$$o_t = \sigma(W_o[h_{t-1}, x_t] + b_o) \tag{3.9}$$

$$h_t = o_t * \tanh(C_t) \tag{3.10}$$

The input gate (i_t) assesses the extent to which incoming data should alter the cell's memory state. Simultaneously, the forget gate (f_t) decides which portions of the cell state are no longer relevant to the task at hand and should thus be discarded. This selective retention and disposal of information ensures that the LSTM cell retains only pertinent data, preventing the dilution of relevant information across the network. The values of the forget gate range from 0 to 1, with higher values indicating data of critical relevance. A value of 0 at the forget gate signifies that the corresponding information is extraneous and should be omitted from the cell state.

On the other hand, the output gate (o_t) determines the influence of the cell state on other cells within the network. This gate controls the extent to which the value within a cell will contribute to the network's output at any given timestep. The operations of these gates are governed by activation functions—the hyperbolic tangent

(tanh) and the sigmoid function. The tanh function scales the cell state, while the sigmoid function, which outputs values between 0 and 1, regulates the gates' opening and closing. The LSTM cell's state is updated through a series of operations involving these gates:

- Input gate: decides values to update.
- Forget gate: determines what to discard from the cell state.
- Output gate: controls which part of the updated cell state is used for the LSTM unit's output activation.

Through this intricate system of gates, LSTMs are able to mitigate the adverse effects of exploding and vanishing gradients, thus maintaining the integrity of the gradient across many layers and time steps. This property makes LSTMs particularly suited for modelling complex phenomena such as solar irradiance, where the ability to remember and selectively forget information is paramount. Therefore, using LSTMs in solar irradiance forecasting provides several advantages. Their ability to retain long-term temporal relationships allows for a more nuanced understanding of sequential patterns in solar irradiance data. This characteristic is particularly beneficial when predicting solar output, which is subject to various temporal influences, such as diurnal and seasonal cycles.

3.4.3 Hybrid NARX-LSTM Model

The hybrid NARX-LSTM architecture synthesizes the distinct features of the NARX neural network with the LSTM's sequential data processing capability to create a robust forecasting model for solar irradiance. This composite model aims to harness the precise nonlinear mapping of NARX and the long-term sequential memory of LSTMs.

The NARX network, serving as the foundation of the hybrid model, takes the lead in forecasting by utilizing its dynamic feedback mechanism. It processes both current and historical data points, employing its distinctive feedback loops to produce an initial forecast. The mathematical representation of the NARX network can be summarized as follows:

$$\hat{y}_{narx}(t) = f\left(W_{narx}\left[\left(y(t-1)\right), \dots, y\left(t-d_y\right), u(t), u(t-1), \dots, u(t-d_u) + b_{narx}\right]\right) \quad (3.11)$$

The LSTM layer is then introduced to refine the NARX output by focusing on minimizing the residuals, $R(t)$. The LSTM network's equations, outlined earlier, enable it to effectively capture and learn from the temporal patterns within the residuals.

$$R(t) = y(t) - \hat{y}_{narx}(t) \quad (3.12)$$

These residuals are then passed to the LSTM network, which seeks to learn a corrective sequence, $\Delta\hat{y}_{lstm}(t)$, to apply to the NARX output:

$$\Delta\hat{y}_{lstm}(t) = LSTM(R(t), h_{t-1}, C_{t-1}) \quad (3.13)$$

The LSTM function represents the internal operations of the LSTM cell, including its gates and state updates, taking the residual at time t, the previous hidden state h_{t-1}, and the previous cell state , C_{t-1}. This approach enables the LSTM network to harness the learning capabilities of NARX, thereby enhancing the pattern recognition in the forecasting system.

The final forecast $\Delta\hat{y}(t)$ from the hybrid NARX-LSTM model is then computed by adjusting the NARX forecast with the corrective sequence from the LSTM:

$$\Delta\hat{y}(t) = \hat{y}_{narx}(t) + \Delta\hat{y}_{lstm}(t) \quad (3.14)$$

To train the hybrid model in a unified manner, a joint loss function can be defined. This loss function, L, not only penalizes the disparity between the actual values and the final forecast from the hybrid model but also include regularization terms to control the complexity of the model:

$$L = \alpha \cdot MSE_{narx} + \beta \cdot MSE_{lstm} + \lambda \cdot (\|W_{narx}\|^2 + \|W_{lstm}\|^2) \quad (3.15)$$

This loss function ensures that during training, both the NARX and LSTM models are optimized to work in harmony, with the regularization terms preventing overfitting by penalizing excessive weights.

The optimization of the hybrid model is performed using a stochastic gradient descent algorithm or one of its adaptive variants. The gradients for the LSTM and NARX parts of the network are computed through backpropagation, considering the dependencies between the two models. The weights and biases of both the NARX and LSTM models are updated iteratively based on the gradients computed from the loss function, L. The update rules can be formally expressed as:

$$W_{narx}^{(new)} = W_{narx} - \eta \frac{\partial L}{\partial W_{narx}} \quad (3.16)$$

$$b_{narx}^{(new)} = b_{narx} - \eta \frac{\partial L}{\partial b_{narx}} \quad (3.17)$$

$$W_{lstm}^{(new)} = W_{lstm} - \eta \frac{\partial L}{\partial W_{lstm}} \quad (3.18)$$

$$b_{lstm}^{(new)} = b_{lstm} - \eta \frac{\partial L}{\partial b_{lstm}} \quad (3.19)$$

Where η is the learning rate, and the partial derivatives represent the gradients of the loss function with respect to the corresponding weights and biases of the NARX and LSTM networks.

The performance evaluation of the forecast system is methodically conducted and documented in this section. Utilized as the primary indicators of accuracy, Root Mean Squared Error (RMSE), Normalized Root Mean Squared Error (nRMSE), and Mean Absolute Error (MAE) are applied to assess the model's predictions against varying weather conditions. Furthermore, the system's performance is contextualized by a comparison with the standalone models.

$$MSE = \frac{1}{n}\sum_{i=1}^{n}(y_i - \hat{y}_i)^2 \tag{3.21}$$

$$RMSE = \sqrt{\frac{1}{n}\sum_{i=1}^{n}(y_i - \hat{y}_i)^2} \tag{3.21}$$

$$nRMSE = 100(\%)\sqrt{\frac{1}{n}\frac{\sum_{i=1}^{n}(y_i - \hat{y}_i)^2}{y_c}} \tag{3.22}$$

The adoption of the NARX neural network in the proposed model is grounded in its proven efficacy in addressing the latching phenomenon and in identifying nonlinear relations. Complementing this, the Long Short-Term Memory (LSTM) network mitigates the vanishing gradient issue, which is crucial for maintaining the model's learning capacity over long sequences. To elucidate the mechanics of the proposed hybrid model, we delineate a four-stage data processing framework as depicted in Figure 3.9.

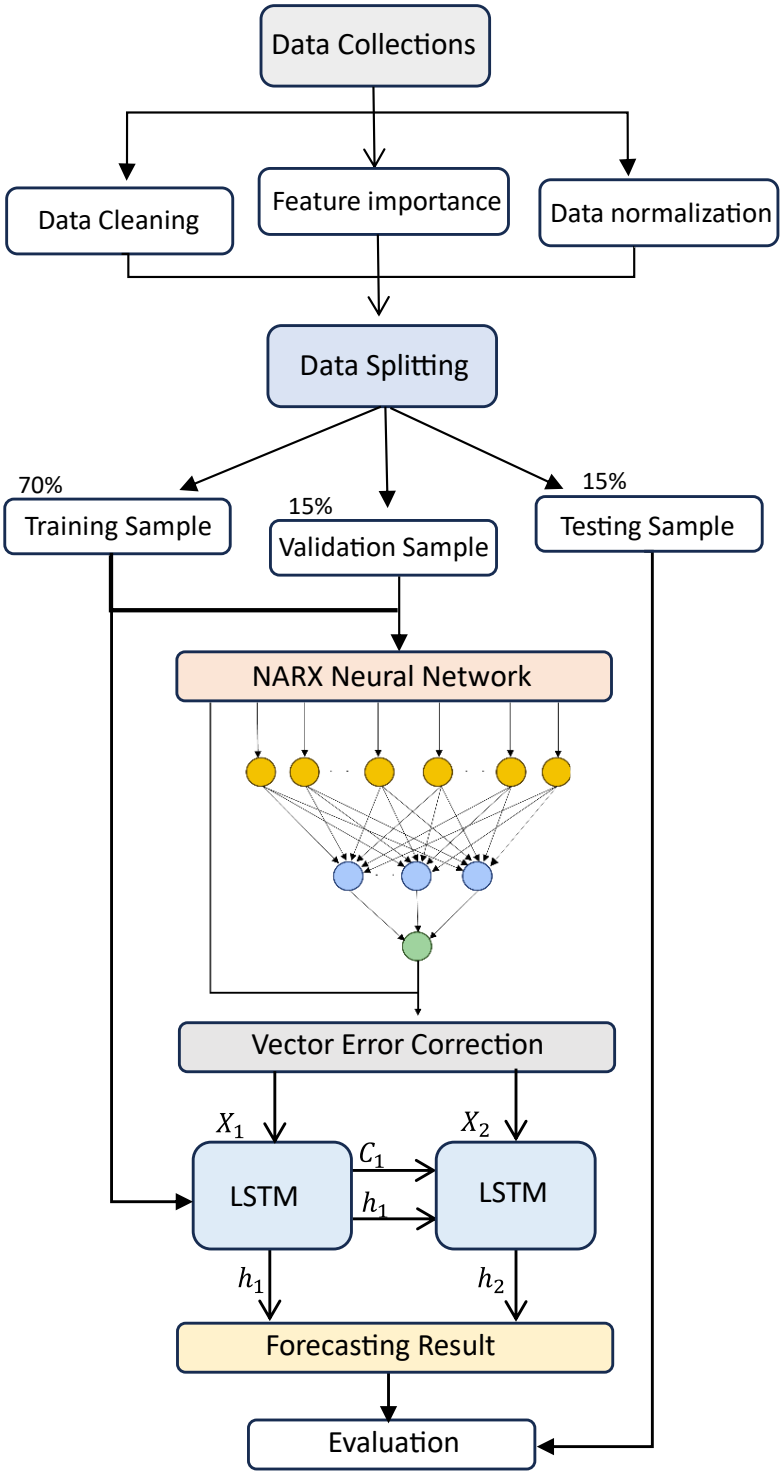

Figure 3.9 The architecture of the proposed model.

3.5 Input Sensitivity Analysis

In the Input Sensitivity Analysis section, a detailed examination is conducted to evaluate the influence of each input parameter on the solar irradiance forecasting model's performance. This analysis plays a crucial role in identifying which weather parameters are most significant in predicting solar irradiance. Techniques such as feature importance ranking and sensitivity testing are employed to discern how variations in input data like air temperature, cloud cover, humidity, and other meteorological factors affect the model's predictions.

The Random Forest algorithm is employed to determine the significance of various weather parameters. This is achieved by establishing a regression-based ensemble model through the Random Forest algorithm which generates a multitude of decision trees (nTrees = 100) to predict the target variable solar irradiance (SI). The algorithm's efficacy hinges on its Out-Of-Bag (OOB) estimator for assessing feature importance, represented by:

$$Feature\ Importance\ (FI) = \sum OOB_{Ccases} = \left(Error_{permuted} - Error_{original}\right) \quad (3.23)$$

Where $Error_{permuted}$ and $Error_{original}$ are the prediction errors on OOB samples before and after permuting each predictor variable. The OOB Mean Squared Error (MSE), is computed as the average squared difference between the observed and predicted GHI values for OOB samples:

$$OOB\ MSE = \frac{1}{N_{OOB}} \sum \left(SI_{permuted} - SI_{original}\right)^2 \quad (3.24)$$

Where is N_{OOB} the number of OOB samples. The OOB error trend across the number of trees is visualized to guide model complexity decisions. This comprehensive methodological approach allows for an in-depth understanding of each weather parameter's influence on the predictive model, thereby optimizing the solar irradiance forecasting.

3.6 Chapter Summary

This chapter has laid the essential foundation for the development and evaluation of a hybrid NARX-LSTM model, targeted at enhancing solar irradiance forecasting. The chapter began with an exploration of the individual components of the model: the Nonlinear Autoregressive with Exogenous Inputs (NARX) and Long Short-Term Memory (LSTM) neural networks. These components were then intricately integrated to form a robust hybrid model capable of capturing the complex dynamics of solar irradiance influenced by various meteorological factors. Detailed data analysis, including a thorough examination of key weather parameters and their relationships with solar irradiance, underpinned the model's development. The preprocessing stage further refined the data, preparing it for effective model training. Additionally, an Input Sensitivity Analysis section was introduced to assess the impact of different input variables on the model's performance, further enhancing its predictive accuracy. This foundational work sets the stage for a comprehensive approach to accurately forecast solar irradiance, a critical factor in optimizing renewable energy systems like microgrids.